Ultrasound-assisted fast encapsulation of metal microparticles in SiO$_2$ via an interface-confined sol-gel method

Youwen Tian, Wei Luo, Yedan Wang, Yun Yu, Wanzhen Huang, Haodong Tang, Yifan Zheng, Zongjian Liu[*]

College of Chemical Engineering, Zhejiang University of Technology, Hangzhou 300014, PR China

A B S T R A C T

Although the traditional Stöber process-based methods are widely used for encapsulation of metal nanoparticles in SiO$_2$, these time-consuming methods are not effective for coating metal microparticles with a uniform SiO$_2$ layer of desired thickness. Herein, an ultrasound-assisted, interface-confined sol–gel method is proposed for fast encapsulation of metal microparticles in SiO$_2$, and the encapsulation of Sn microparticles is chosen as an example to illustrate its feasibility. The proposed method involves covering metal microparticles with liquid films that contain water, alcohol, surfactant (Span-80) and catalyst (NH$_4$F) and then ultrasonically dispersing these particles into cyclohexane, where tetraethylorthosilicate (TEOS) is added. To ensure the hydrolysis-condensation reactions of TEOS occurring at the particle-cyclohexane interface so that the formed SiO$_2$ is coated on the particles, the microparticles should be well dispersed into cyclohexane with the liquid films being not broken away from their surfaces. It is found that the assistance of probe sonication and the addition of surfactant are crucial to achievement of a good dispersion of metal microparticles in cyclohexane. And using high-viscosity alcohol (namely glycerol), controlling the volume ratio of water to alcohol and the amount of water, and choosing a suitable ultrasonic power are essential for preventing the formation of free SiO$_2$ (namely SiO$_2$ that is not coated on the particles), which is a result that the liquid films escape from the particle surfaces under ul-trasonic cavitation. Our results have also revealed that the thickness of SiO$_2$ layer can be adjusted by changing the reaction time or the total amount of water. In particular, the thickness of SiO$_2$ layer can be easily raised by simply repeating the encapsulation procedure. Compared with the traditional Stöber process-based methods, the proposed method is time-saving (reaction time: about 30 min vs. more than 12 h) and extremely effective for coating microparticles with a continuous, uniform SiO$_2$ layer of desired thickness.

1. Introduction

SiO$_2$-coated metal particles are a class of materials widely used in many fields including colloid, bioscience and medical industry, catalysis, and thermal energy storage-related science [1,2]. The sur-face SiO$_2$ layer, for example, allows manipulation of the interaction potential and makes it possible to disperse metal colloidal particles in many solvents ranging from very polar to nonpolar [3]. SiO$_2$ shell also allows core nanoparticle to be biocompatible and easily bioconjugated with functional groups, which is necessary for biomedical, diagnostic and therapeutic applications [2,4,5]. In the field of catalysis, encap-sulating the ultrasmall-sized metal particles in SiO$_2$ has been recently recognized as a promising technique to address sintering and coke deactivation in high-temperature catalytic reactions such as

methane oxidation, dry reforming of methane, and carbon monoxide oxidation [6–8].

While SiO$_2$-coated metal nanoparticles have been extensively investigated [1–8], much less attention is paid to SiO$_2$-coated metal micro-sized particles. Currently, the work on the SiO$_2$-coated metal microparticles mainly focuses on their application in thermal energy storage-related science because the SiO$_2$-coated metal phase-change materials (PCM), with a higher heat storage density compared to the PCM nano-capsules, can not only be used as a mode of heat transfer and transport flux but also can be mixed with other substances to form multifunctional materials [9–13]. In our group, we are interested in the use of SiO$_2$-coated metal PCM microparticles as the catalyst support to control the temperature of catalyst bed in highly exothermic gas–solid catalytic reactions. To avoid the leakage of PCM and have the ability for

* Corresponding author.
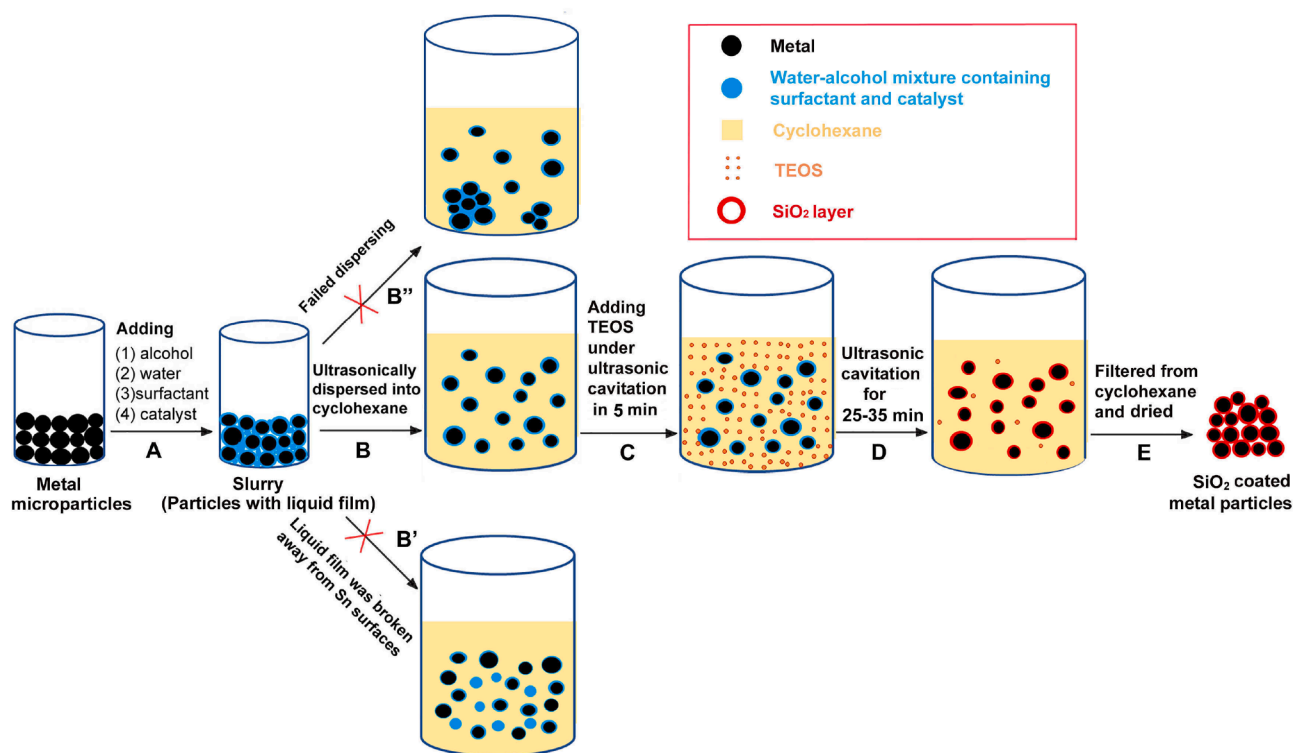 *E-mail address:* zjliu@zjut.edu.cn (Z. Liu).

Fig. 1. Scheme for ultrasound-assisted fast encapsulation of micro-sized metal particles in SiO$_2$ via an interface-confined sol–gel method.

accommodation of the active component, a continuous, uniform SiO$_2$ layer with a desired thickness is essential for their practical applications. So far, a wide variety of methods have been developed for SiO$_2$ coating [1,14–16], and the Stöber-based processes [17] are commonly used. The so-called Stöber method refers to the growth of SiO$_2$ shells by addition of tetraethoxysilane (TEOS) to the dispersion of core particles in an alcohol-ammonia mixture. To effectively grow homogenous SiO$_2$ shells on the cores, surface modification of the metal cores with coupling

agents, surfactants or polymers are generally required to increase the compatibility of the core surface with SiO$_2$ and the stability of metal cores in alcohol mediums. For the metal particles with a size greater than 1 μm, however, their settling in alcohol-based mediums is inevitable. As a result, while these time-consuming Stöber process-based methods (the reaction time is often more than 12 h) are extremely effective for coating metal nanoparticles with a SiO$_2$ layer of desired thickness [1,18,19], they are much less useful for encapsulating metal
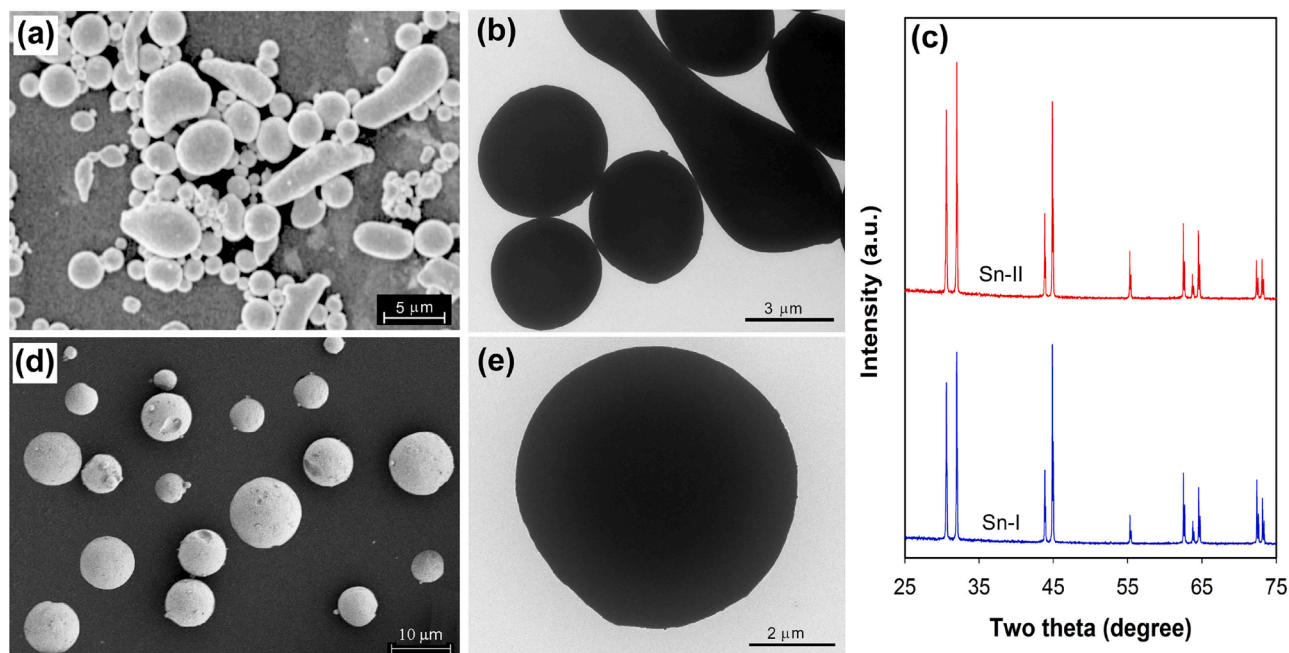

Fig. 2. (a) SEM image of Sn-I, (b) TEM images of several Sn-I particles, (c) XRD patterns of both Sn-I and Sn-II, (d) SEM image of Sn-II, and (e) TEM image of a Sn-II particle.
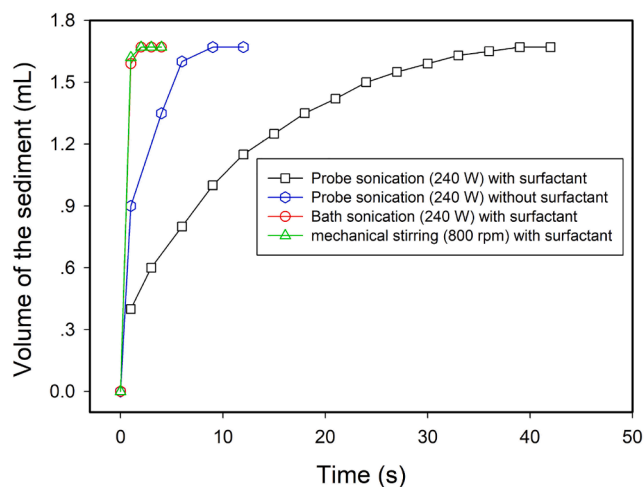
Fig. 3. The volume of the sediment as a function of time after dispersing under different conditions.

microparticles in SiO$_2$. Wang and Harrison, for instance, reported a study of coating Fe particles (~1μm in size) via a gelatin-assisted Stober method [20]. Based on their transmission electron microscopy (TEM) results, the SiO$_2$ layer is thin and discontinuous. Therefore, fast encapsulation of metal microparticles with a continuous, uniform SiO$_2$ layer of desired thickness currently remains a great challenge.

In this work, we present an investigation on ultrasound-assisted fast encapsulation of micro-sized metal particles in SiO$_2$ via an interface-confined sol–gel method. As illustrated in Fig. 1, this new method involves covering microparticles with liquid films that contain water, alcohol, surfactant (Span-80) and catalyst (NH$_4$F) and then ultrasonically dispersing these particles into cyclohexane, where tetraethylorthosilicate (TEOS) is added. To illustrate its feasibility, Sn microparticles were used as the cores in this study. Interest in the synthesis of SiO$_2$ encapsulated Sn microspheres is based on the following consideration. Sn has a melting point of about 231 °C, a value close to the reaction temperature of low-temperature Fischer–Tropsch synthesis, a highly exothermic gas–solid catalytic reaction. Since SiO$_2$ is a widely-used support of cobalt catalyst in Fischer–Tropsch synthesis, SiO$_2$ encapsulated Sn microspheres, serving as both PCM and supports of Co catalysts,
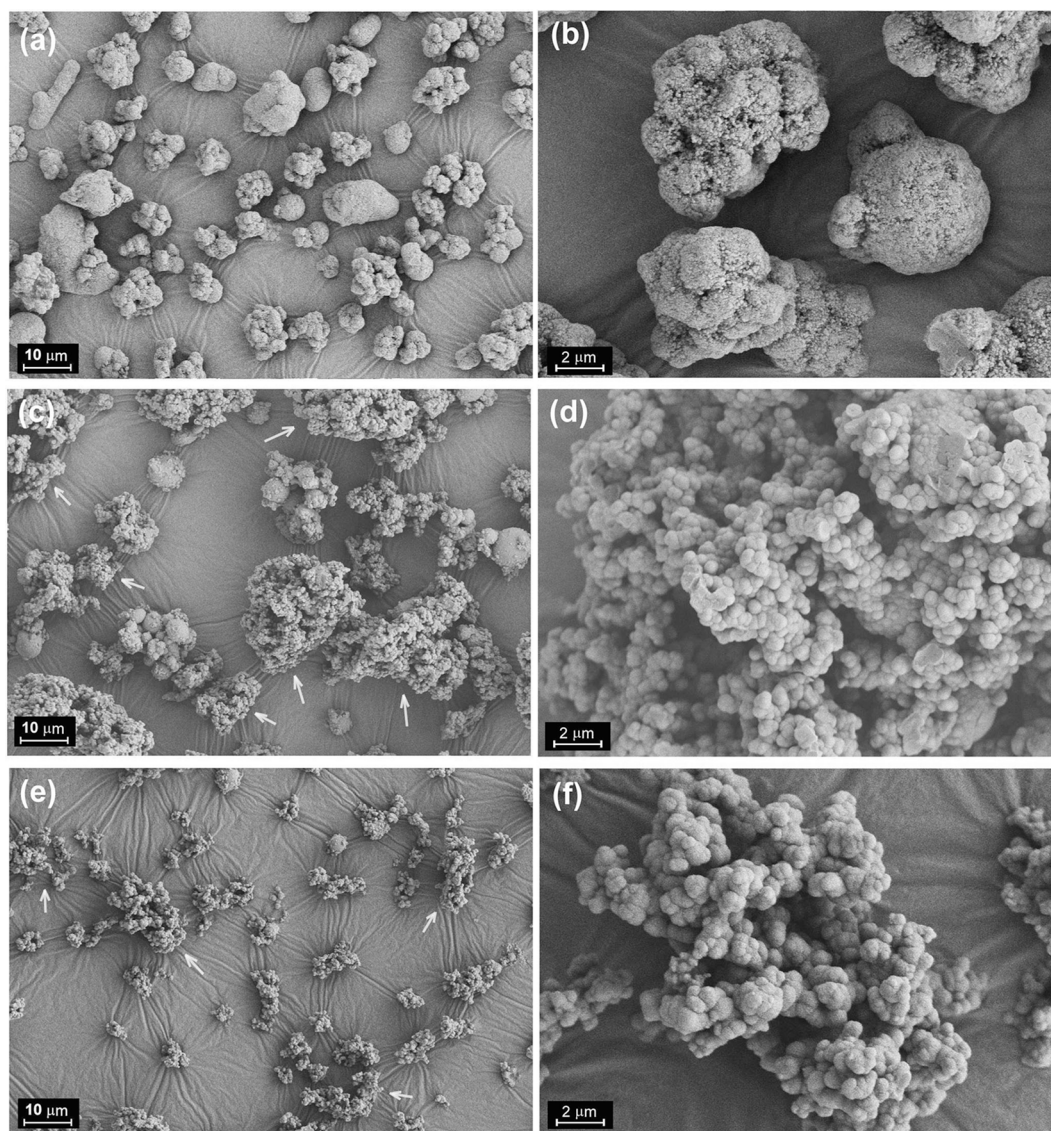

Fig. 4. SEM image of the product obtained via the interface-confined sol–gel method under different conditions: (a. b) probe sonication (240 W) in the absence of surfactant, (c,d) mechanical stirring (800 rpm) in the presence of surfactant, and (e,f) bath sonication (240 W) in the presence of surfactant. Other experimental conditions: volume ratio of glycerol to water = 4:1, the amount of water = 0.048 mL, reaction time = 40 min, and Sn type is Sn-I.
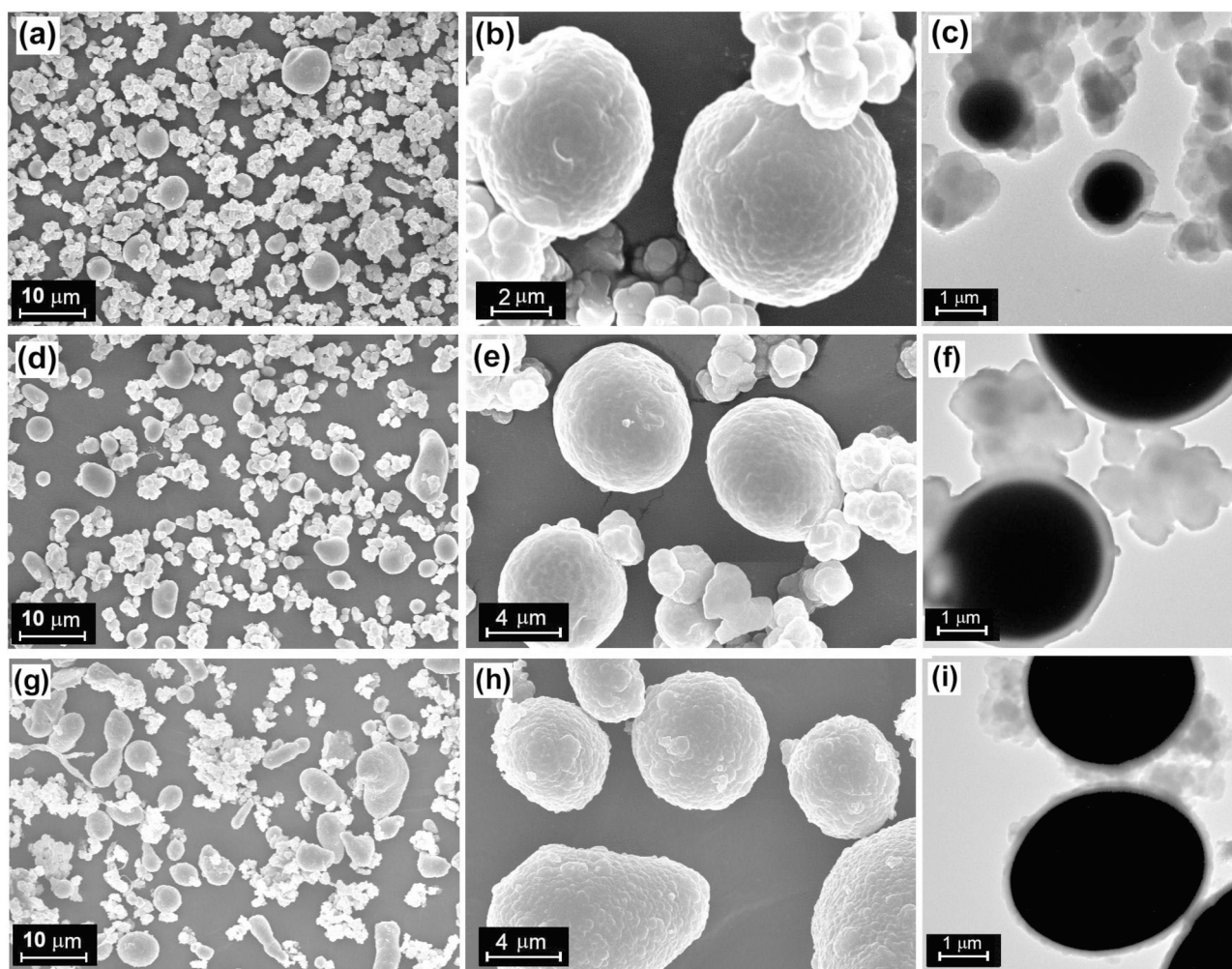
Fig. 5. SEM and TEM images of the products obtained by using different alcohols: (a-c) ethanol, (d-f) ethylene glycol, and (g-i) glycerol. Other experimental conditions: ultrasonic power = 240 W, volume ratio of alcohol to water = 1:1, the amount of water = 0.048 mL, reaction time = 40 min, and Sn type is Sn-I.

are potential candidates for latent heat storage in Fischer–Tropsch synthesis. Although the proposed interface-confined sol–gel method is a little similar to the reverse microemulsion method for encapsulation of metal nanoparticles in SiO₂ [19], the former is significantly different from the latter in several ways. (i) Ultrasonic cavitation is mandatorily required. (ii) High-viscosity alcohol (namely glycerol) need be used as the hydrolysis inhibitor. (iii) The total amount of water and alcohol must be strictly controlled. (iv) Small amount of NH_4F, rather than ammonia, serves as the catalyst for fast gelatination. As a result, our experimental result will show that, in contrast to the reverse microemulsion method, this new method is time-saving and extremely effective for coating micro-sized metal particles with a continuous, uniform SiO₂ layer of desired thickness.

2. Materials and methods

2.1. Materials and chemicals

All chemicals were of analytical grade and used as received. Except for poly-(vinylpyrrolidone (PVP, 1300000) (purchased from Maclin Biochemical Technology Co., Ltd.), ethanol (Anhui Ante Food Co. Ltd) and ammonia (25–30 wt%, purchased from Hangzhou Longshan Fine Chemical Co., Ltd.), and Sn microparticles (purchased from Shanghai Zhili Metallurgical Sales Department, denoted as Sn-I), all other reagents were obtained from Aladdin Chemical Reagent Co., Ltd.

Besides the purchased Sn microparticles, Sn microparticles was also prepared by a molten salt-based metal emulsion method (denoted as Sn-II). Typically, about 2.23 g bulk Sn particles was firstly added into a quartz tube (inner size $\varphi\,45 \times 150$ mm) containing 7.65 mL molten LiCl–KCl–CsCl eutectic (melting point: ~270 °C) at 300 °C under argon gas protection, and then the mixture was emulsified via ultrasonic cavitation (20 KHz, 1080 W, 3 s interval between every 2 s duty) for about 10 min with the distance between the sonotrode tip (φ20 mm) and the molten salt-metal interface being about 8 mm. The resulting emulsion was quickly cooled to room temperature so that the Sn droplets could be confined in the salt matrix. The chloride salts were removed by dissolving the salt-metal mixture in deionized water. After removal of the salts, the solid product was washed with deionized water and then dried in vacuum at 60 °C for 5 h.

2.2. Stability of dispersion of Sn microparticles in cyclohexane and encapsulation of microsized Sn particles in SiO₂

Stability of dispersion of Sn microparticles in cyclohexane. 1.4 g Sn-I, 1.67 mL glycerol solution (20 vol% water in glycerol), and 0.0560 g Span-80 (if needed) were added into a precisely calibrated plastic tube, and the mixture was stirred until blended. 10 mL cyclohexane was added into the formed slurry, and the slurry was then dispersed into cyclohexane by mechanical stirring (800 rpm), bath sonication (240 W), or probe sonication (240 W, duty ratio 3/5, sonotrode tip diameter = 10
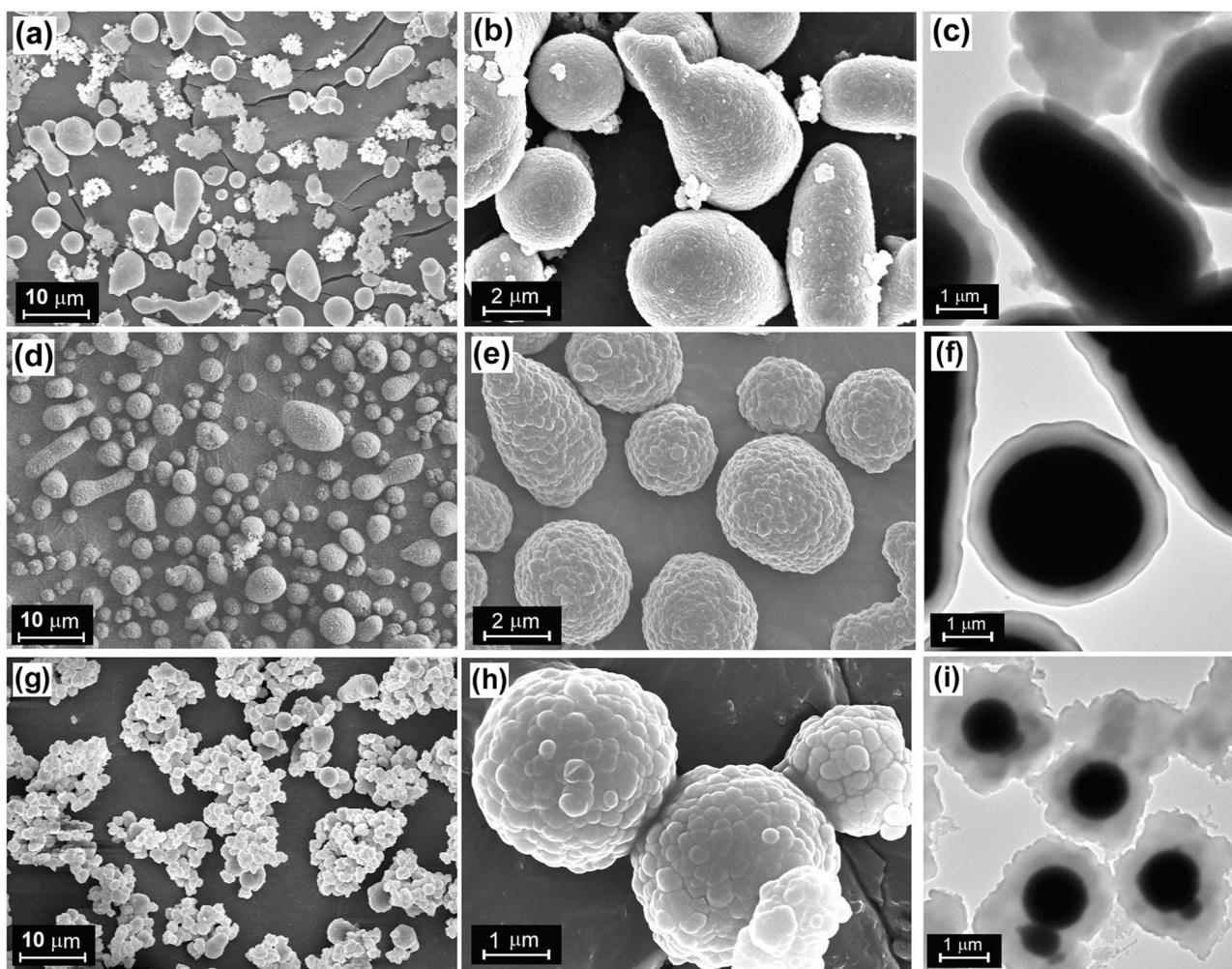
Fig. 6. SEM and TEM images of the products obtained by using different volume ratio of glycerol to water: (a-c) 2:1, (d-f) 4:1, and (g-i) 6:1. Other experimental conditions: ultrasonic power = 240 W, the amount of water = 0.048 mL, reaction time = 40 min, and Sn type is Sn-I.

mm, the distance between the sonotrode tip and the cyclohexane-slurry interface is ~ 8 mm) for 2 min. After dispersing, the volume of the sediment was recorded as a function of time.

Ultrasound-assisted fast encapsulation via an interface-confined sol–gel method. Typically, 0.20 g Sn microparticles, a given amount of NH_4F aqueous solution (the molar ratio of water to TEOS is fixed at about 2.5:1 and the molar ratio of NH_4F to TEOS is fixed at about 0.01: 1), a given amount of alcohol, and about 0.008 g Span-80 were added into a plastic tube, and the mixture was stirred until blended. 10 mL cyclohexane was added into the formed slurry, and then the tube was placed into a water bath to prevent overheating due to ultrasonic cavitation. The Sn-containing slurry was dispersed into cyclohexane by probe sonication (duty ratio 3/5, sonotrode tip diameter = 10 mm, the distance between the sonotrode tip and the cyclohexane-slurry interface is ~ 8 mm) for 2 min. After dispersing, a given amount of TEOS was added dropwise into the tube under ultrasonic cavitation in 5 min. To complete the hydrolysis-condensation reactions of TEOS, the ultrasonic cavitation lasted typically for 25–35 min. After reaction, the solid product was collected by centrifugation (5000 rpm). The obtained product was then washed with water and ethanol and dried under vacuum.

For comparison, PVP-assisted approach [18] and reverse micro-emulsion method [19] were also employed to encapsulate Sn micro-particles in SiO_2. (i) **PVP-assisted approach**. About 0.13 g PVP was dissolved in 8.7 mL of water, and then 0.2 g Sn microparticles were added under stirring (600 rpm). After stirring for 24 h at room

temperature, the PVP-stabilized particles were obtained by centrifugation (5000 rpm). The PVP-stabilized particles were redispersed in an 8.63 mL ethanol-based solution containing 4.2 vol% ammonia (29.3 wt %NH_3 in water), and a 2.3 mL TEOS solution (10 vol% in ethanol) was added under stirring (600 rpm). The reaction mixtures were then stirred for another 12 h. After reaction, the product was treated by the same procedure as that via interface-confined sol–gel method. (ii) **Reverse microemulsion method**. 0.01 g of Sn powder was dispersed in 6 mL cyclohexane. 0.35 mL of Span-80 was added to the above mixture, and a 0.2 mL of ammonia solution (29.4 wt% in water) and 20 μL of TEOS were then added consecutively under stirring. After 5 h of reaction at room temperature, another 200 μL of TEOS was added and the reaction lasted for another 24 h. After reaction, the product was treated by the same procedure as that via interface-confined sol-–gel method.

2.3. Characterization

The morphology of the samples was examined using a scanning electron microscope (SEM, Hitachi S-4700) operating at 15 kV. The phase composition was analyzed by X-ray diffraction (XRD), which was performed on a Thermo ARL XTRA X-ray diffractometer (Thermo Fisher Scientific) using Cu K α X-ray source. The microstructure investigations were performed with a Tecnai G2 F30 S-Twin transmission electron microscopy operating at 300 kV or a FEI Talos-S transmission electron microscope operating at 200 kV.
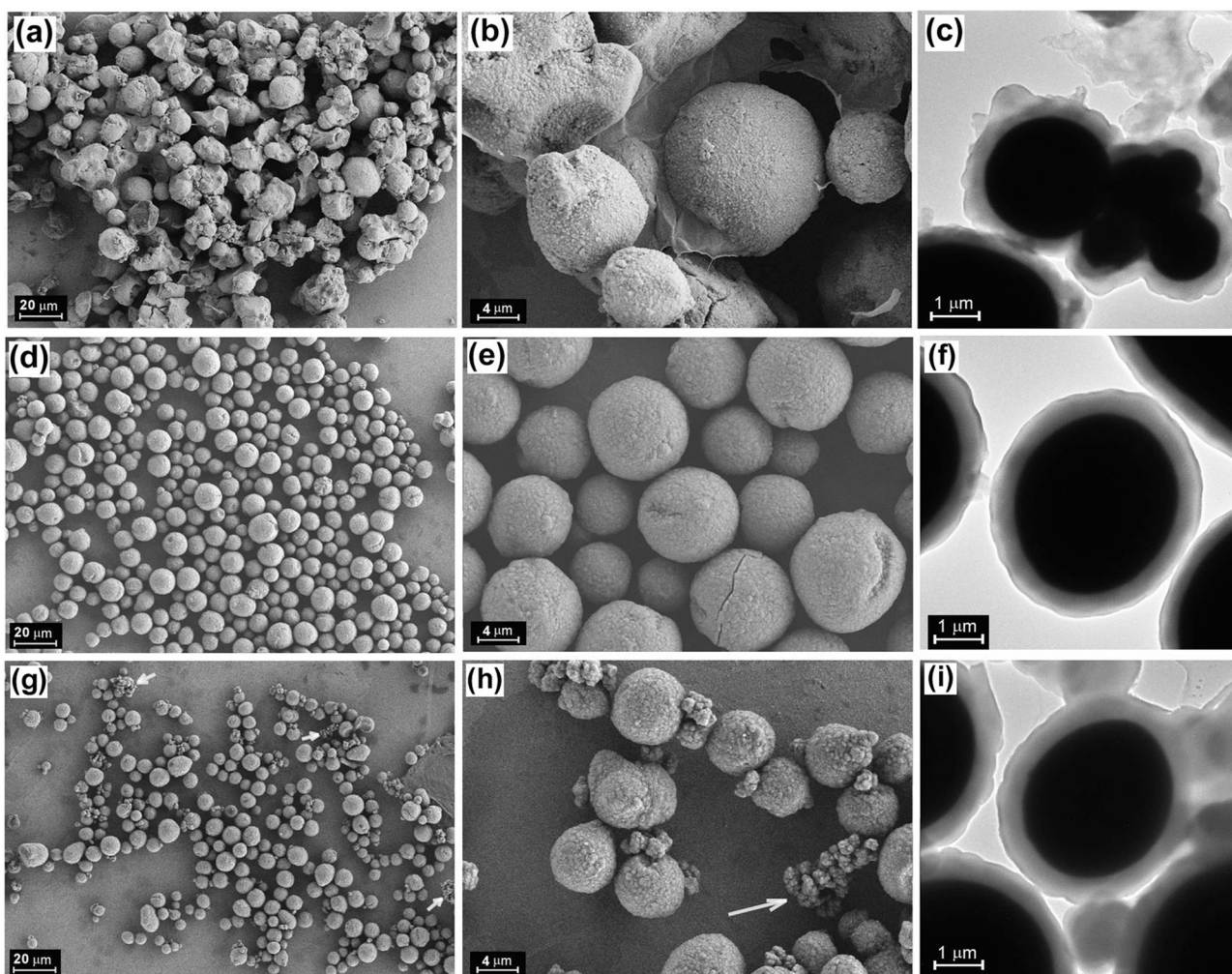
Fig. 7. SEM and TEM images of the products obtained under different ultrasonic powers: (a-c) 120 W, (d-f) 240 W, and (g-i) 360 W. Other experimental conditions: volume ratio of glycerol to water = 4:1, the amount of water = 0.048 mL, reaction time = 40 min, and Sn type is Sn-II.

3. Results and discussion

3.1. Morphology and microstructure of microsized Sn particles

Two types of microsized Sn particles were used in our experiments. One was purchased Sn-I. As shown in Fig. 2a and 2b, the purchased sample contains both spherical particles and irregular shaped particles and the size of these particles ranges from about 1 μm to more than ten micrometers. The XRD patterns of the sample (Fig. 2c) confirms that these particles are Sn because the diffraction peaks at 2θ of 30.6°, 32.0°, 43.9°, 44.9°, 55.4°, 62.5°, 63.8°, 64.6°, 72.4° and 73.1° can all be indexed to metal Sn with a tetragonal structure (space group I41/amd, JCPDS 04–0673) and correspond to the diffractions of (200), (101), (220), (211), (301), (112), (400), (321), (420) and (411) planes, respectively. The unit cell parameters estimated from the XRD patterns are: a = 0.5835 nm, b = 0.5835 nm and c = 0.3183 nm. Another was Sn-II prepared by a molten salt-based metal emulsion method. Similar to Sn-I, all the peaks appearing in the XRD patterns of Sn-II can be indexed to metal Sn with a tetragonal structure (space group I41/amd, JCPDS 04–0673). The lattice parameters for Sn-II calculated are: a = 0.5840 nm, b = 0.5840 nm and c = 0.3185 nm, indicating a slight lattice expansion compared to Sn-I. As can be seen from its SEM image (Fig. 2d), Sn-II is composed of spherical Sn particles, and the diameter of the small particles is several micrometers and that of the big particles is more than ten micrometers. The TEM image of a particle (Fig. 2e) suggests that the particle is solid, rather than hollow.

3.2. Ultrasound-assisted fast encapsulation of microsized Sn particles in SiO₂

Accoring to the encapsulation procedure shown in Fig. 1, the occurrence of the hydrolysis and condensation reactions of TEOS at the particle-cyclohexane interface is cruial to encapsulation of microsized Sn particles in SiO₂. To ensure the ocuurence of this interface-confined reaction, two conditions must be satisfied. (i) The liquid film-covered Sn microparticles need be well dispersed intocyclohexane. (ii) The liquid film should not be broken away from the surfaces of Sn microparticles and thus liquid droplets, which will lead to the formation of free SiO₂ (namely SiO₂ that is not coated on the Sn particles), are absent in cyclohexane. In this section, therefore, we will first clarify the conditions for the formation of a dispersion of Sn microparticles in cyclohexane and illustrate the encapsulation results obtained from the failed dispersing. Then the factors which may give rise to the formation of liquid droplets in cyclohexane will be investigated to reduce the amount of free SiO₂. Finally, we will address how to adjust the thickness of SiO₂ layer.

3.2.1. Dispersing liquid film-covered Sn microparticles into cyclohexane

Unlike pure metal microparticles, the Sn microparticles are covered by a liquid layer containing both water and high-viscosity alcohol (e.g. glycerol) that are insoluble in cyclohexane. As a result, these liquid film-covered Sn particles are actually agglomerated in cyclohexane before dispersing. A good dispersion means that single liquid film-covered Sn
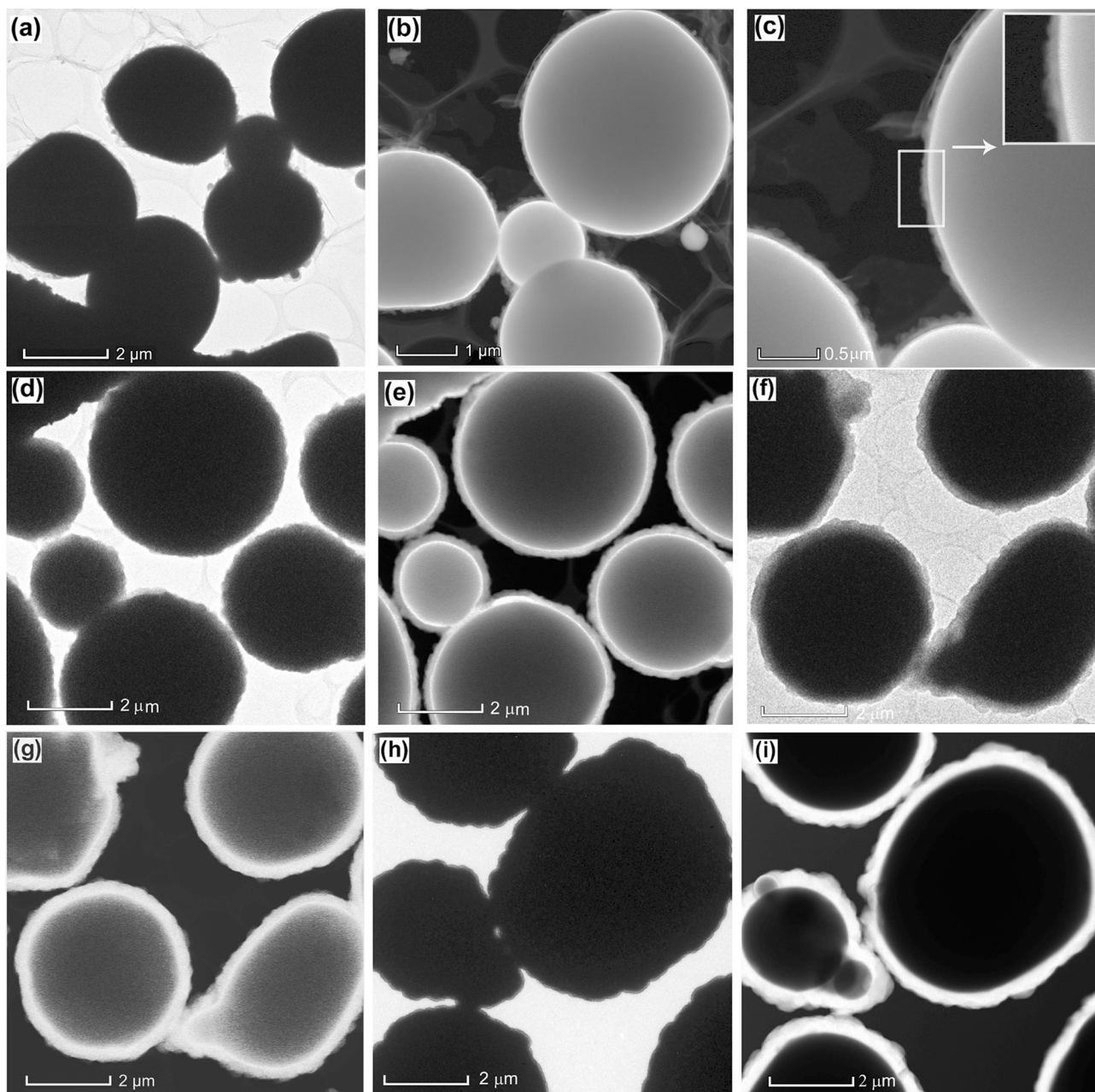
Fig. 8. TEM and STEM images of the products obtained after different reaction durations: (a-c) 10 min, (d,e) 20 min, (f,g) 30 min, and (h,i) 40 min. Inset in (c) is an enlarged version of the squared region. Other experimental conditions: ultrasonic power = 240 W, volume ratio of glycerol to water = 4:1, the amount of water = 0.048 mL, and Sn type is Sn-II.

particles, rather than the agglomerated particles, are dominantly present in cyclohexane by successful deagglomeration of these liquid film-covered Sn microparticles, whereas a bad dispersion hints that these liquid film-covered Sn microparticles are not deagglomerated or partially deagglomerated. Since the agglomerated particles are easier to settle down than the single dispersed particles in the presence of gravitational force, we can record the volume of the sediment as a function of time after dispersing to evaluate whether a dispersion is good or not. Fig. 3 presents the volume of the sediment as a function of time after dispersing under different conditions. It is clear that the addition of surfactant and the assistance of probe sonication are essential for achieving a good dispersion of Sn microparticles in cyclohexane. Without surfactant, the rapid settling of Sn particles indicates that the agglomerated microparticles is difficult to be deagglomerated. Similar phenomenon can also be observed in the presence of surfactant when

bath sonication or mechanical stirring, rather than probe sonication, is applied. As illustrated in Fig. 4, the failed dispersing has a significantly negative impact on the product obtained via the interface-confined sol–gel method. The product obtained under probe sonication in the absence of surfactant is composed of agglomerated microparticles (Fig. 4a and 4b), a result from the fact the without surfactant probe sonication cannot efficiently breaks particle agglomerates into single dispersed particles. Besides the agglomerated Sn microparticles, the products obtained under mechanical stirring (Fig. 4c and 4d) or bath sonication (Fig. 4e and 4f) in the presence of surfactant contain large amount of free SiO_2 sub-microspheres which are severely aggregated (indicated by white arrows). This implies that both mechanical stirring and bath sonication tend to break the liquid films away from the surfaces of Sn microparticles and the hydrolysis-condensation reactions of TEOS occurring in the resulting liquid droplets lead to the formation of these
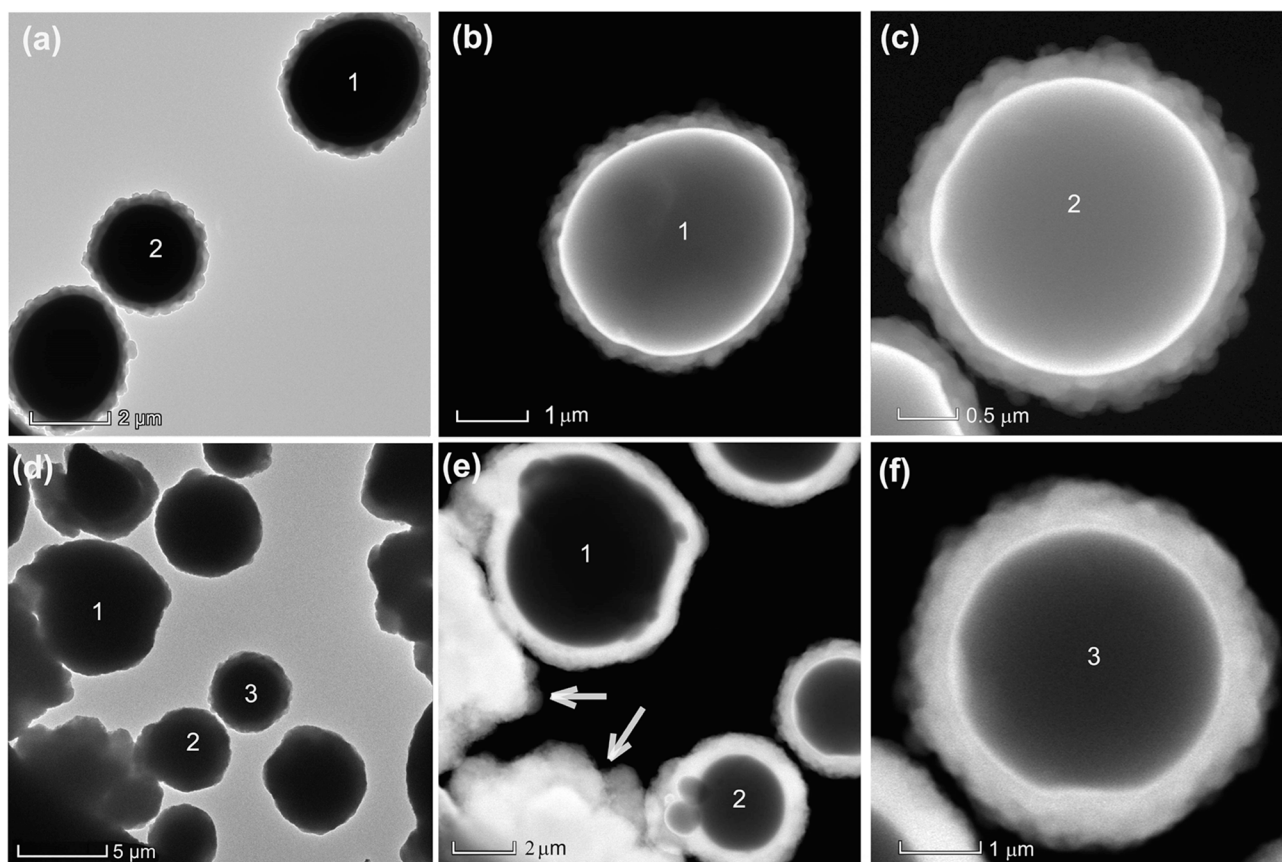
Fig. 9. TEM and STEM images of the products obtained in the presence of different amounts of water: (a-c) 0.032 mL, and (d-f) 0.064 mL. Other experimental conditions: ultrasonic power = 240 W, volume ratio of glycerol to water = 4:1, reaction time = 40 min, and Sn type is Sn-II.

aggregated SiO_2 sub-microspheres. Therefore, the application of probe sonication in the presence of surfactant was chosen for further study.

3.2.2. Reducing the amount of free SiO_2

In order to obtain a SiO_2-encapsulated sample of high quality, the amount of free SiO_2 in the sample must be reduced. The formation of free SiO_2 is a result of occurrence of the hydrolysis-condensation reactions of TEOS in water-alcohol droplets, rather than at the particle-cyclohexane interface. These water-alcohol droplets originate from the liquid films that escape from the surfaces of Sn microparticles under ultrasonic cavitation (see Step B' in Fig. 1). To ensure that the water-alcohol films are firmly adhered to the particle surfaces under ultrasonic cavitation, we try to raise the viscosity of the water-alcohol films by using high-viscosity alcohols. Therefore, although ethanol (dynamic viscosity η = 1.2 mPa.s at 20 °C) is commonly used as the hydrolysis inhibitor in the synthesis of SiO_2 via sol–gel method, ethylene glycol (η = 21.4 mPa.s at 20 °C), especially glycerol (η = 1487 mPa.s at 20 °C), was also employed in this study. Fig. 5 presents the SEM and TEM images of the products obtained by using different alcohols. It is clear that the use of ethanol leads to the formation of large amount of free SiO_2 particles which are aggregated (Fig. 5a and 5b). The TEM image of the product confirms that there exists lots of free SiO_2 particles despite that Sn microparticles are coated with a layer of SiO_2 (Fig. 5c). As indicated by the SEM and TEM images of the product (Fig. 5d-f), it seems that the replacement of ethanol with ethylene glycol has no obvious impact on the amount of free SiO_2 probably because the viscosity of the ethylene glycol–water films is still too low to prevent the films from escaping from the metal particle surfaces. However, the amount of free SiO_2 in the product is noticeably reduced when glycerol is used (Fig. 5g-i). These observations demonstrate that raising the viscosity of the water-alcohol films by using glycerol as the

hydrolysis inhibitor can improve the adhesion of the film to the metal microparticles.

Although the use of glycerol may greatly reduce the amount of free SiO_2, a lot of free SiO_2 is still present in the product. We speculate that the amount of water in the liquid films is still too high and thus the viscosity of the water-glycerol film is not high enough to completely prevent the films from escaping from the metal particle surfaces. Therefore, the volume ratio of glycerol to water is raised with the amount of water being kept unchanged. As shown in Fig. 6a-c, when the volume ratio of glycerol to water is changed from 1:1 (Fig. 5g-i) to 2:1, no obvious change in the amount of free SiO_2 in the product can be observed. However, when the volume ratio of glycerol to water is further raised to 4:1, almost no free SiO_2 is present in the product (see Fig. 6d and 6e) and the TEM image of the product indicates that the particles are coated with a layer of SiO_2 (Fig. 6f). It should be pointed out that a very high volume ratio of glycerol to water (e.g. 6:1 or above) is not favorable for reducing the amount of free SiO_2. As illustrated in Fig. 6g-i, when the volume ratio of glycerol to water is raised to 6:1, many free SiO_2 particles reappears in the product probably because the liquid films are too thick to prevent themselves from escaping from the metal particle surfaces.

The above investigation shows that raising the viscosity of the water-alcohol films by using glycerol as the hydrolysis inhibitor and controlling the volume ratio of glycerol to water can greatly reduce the amount of free SiO_2. However, since the formation of water-alcohol droplets originate from the liquid films that are broken away from the surfaces of Sn microparticles under ultrasonic cavitation, the ultrasonic power is also expected to play an important role. Therefore, to ensure that the water-alcohol film is firmly adhered to the particle surface under ultrasonic cavitation, a suitable ultrasonic power should be chosen. Fig. 7 presents the SEM and TEM images of the products obtained via the
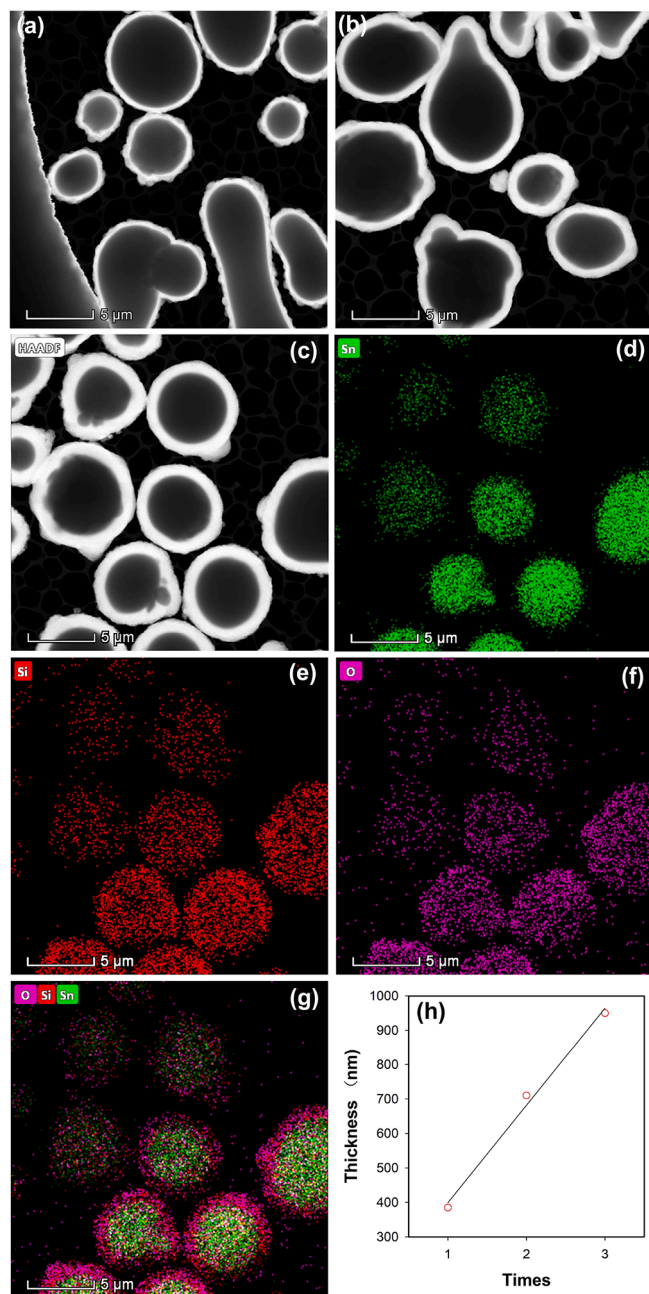
Fig. 10. STEM images of the products obtained via the interface-confined sol–gel method with different encapsulation times: (a) 1, (b) 2 and (c) 3. The element mappings of the corresponding product in (c) are shown in (d-g). Plot of the thickness of SiO$_2$ layer as a function of encapsulation times is shown in (h). Experimental conditions for each encapsulation: ultrasonic power = 240 W, volume ratio of glycerol to water = 4:1, the amount of water = 0.048 mL, reaction time = 40 min, and Sn type is Sn-I.

interface-confined sol–gel method under different ultrasonic powers. At an ultrasonic power of 120 W, the agglomerated microparticles are present in the product (Fig. 7a and 7b) and the TEM image confirms the presence of the agglomerated microparticle coated with a layer of SiO$_2$ (Fig. 7c). The result suggests that probe sonication with a low ultrasonic power cannot efficiently breaks particle agglomerates into single dispersed particles. When the ultrasonic power is raised to 240 W, the phenomenon of particle aggregation disappears and almost no free SiO$_2$ is observed with each particle being encapsulated in SiO$_2$ (Fig. 7d-f). However, when the ultrasonic power is raised to 360 W, free SiO$_2$ appears (indicated by arrows in Fig. 7g and 7 h). The result can be

explained by the fact that a higher power delivered to an ultrasonic transducer can produce a stronger amplitude of ultrasonic waves by which the water-glycerol films may be more easily broken away from the surfaces of Sn microparticles.

3.2.3. Adjusting the thicnkness of the SiO$_2$ layer

Encapsulated metal microparticles with a desired thickness of SiO$_2$ layer is essential for their practical applications. For example, the use of SiO$_2$-coated metal PCM microparticles as the catalyst support to control the temperature of catalyst bed in highly exothermic gas–solid catalytic reactions, the thickness of SiO$_2$ layer should be thick enough to avoid the leakage of PCM and have the ability for accommodation of the active component. Therefore, controlling the thickness of SiO$_2$ layer is of great importance. Since the formation of free SiO$_2$ can be prevented by choosing suitable experimental conditions, the thickness of SiO$_2$ layer is mainly depends on the amount of TEOS consumed. In our experiments, the molar ratio of TEOS to water is kept at a fixed value (namely about 1:2.5), and thus the amount of TEOS consumed is related to depends on the reaction time and the amount of water added. Fig. 8 presents the TEM and STEM images of the products obtained after different reaction durations. After 10 min reaction under ultrasonic cavitation (Fig. 8a-c), a very thin, continuous SiO$_2$ layer (less than 100 nm) can be observed on the surface of Sn particles (see inset in Fig. 8c), indicating that most TEOS is not consumed even in the present of catalyst of NH$_4$F. However, when the reaction time is prolonged to 20 min, a uniform SiO$_2$ layer with thickness of about 200 nm is coated on the microparticles (Fig. 8d-e). As shown in Fig. 8f-g, the thickness of SiO$_2$ layer can be raised to a value close to 400 nm when the reaction time is increased to 30 min. However, only a slight rise in the thickness of SiO$_2$ layer is observed when further prolonging the reaction time to 40 min, indicating that most TOES is consumed after 30 min reaction. These results suggest that we can reduce the thickness of SiO$_2$ layer by properly shortening the reaction time, but the shortcoming is that only part of TEOS is consumed and thus some TEOS is wasted.

The drawback present in the case of shortening reaction time can be overcome by choosing another method, namely reducing the amount of water. Fig. 9 presents the TEM and STEM images of the products obtained by adding different amounts of water. As shown in Fig. 9a-c, the thickness of SiO$_2$ layer is close to 300 nm when the amount of water is reduced from 0.048 mL to 0.032 mL. A rise in the amount of the water can lead to an increase in the thickness of SiO$_2$ layer. For example, the thickness of SiO$_2$ layer is more than 600 nm if the amount of water is raised to 0.064 mL. As indicated by arrows in Fig. 9e, however, a lot of free SiO$_2$ appears in the product. This hints that the liquid films are too thick and thus may escape from the surface of the microparticles (namely form liquid droplets in cyclohexane) under ultrasonic cavitation.

Although reducing the reaction time or the amount of water can adjust the thickness of the SiO$_2$ layer, it is difficult to raise the thickness of SiO$_2$ layer to more than 600 nm without formation of free SiO$_2$ via these methods. However, we find that the thickness of the SiO$_2$ layer can be easily raised by simply repeating the encapsulation procedure. Fig. 10a-c present the STEM images of the products obtained via the interface-confined sol–gel method with different encapsulation times, and the energy dispersive X-ray spectrum (EDS) element mappings of the corresponding product in Fig. 10c are shown in Fig. 10d-g. Several features can be found from Fig. 10. (i) Based on the element mappings, the cores with dark contrast in STEM images are Sn and the shells with the bright contrast are SiO$_2$. (ii) All Sn microparticles, whether spherical shaped or irregular shaped, are coated with a layer of SiO$_2$. (iii) The thickness of the SiO$_2$ layer increases almost linearly with the encapsulation times (Fig. 10h), namely increases from around 400 nm to about 1 μm after three times encapsulation. These results suggest that the proposed method is extremely effective for encapsulating microparticles of different shapes with a uniform SiO$_2$ layer of desired thickness.
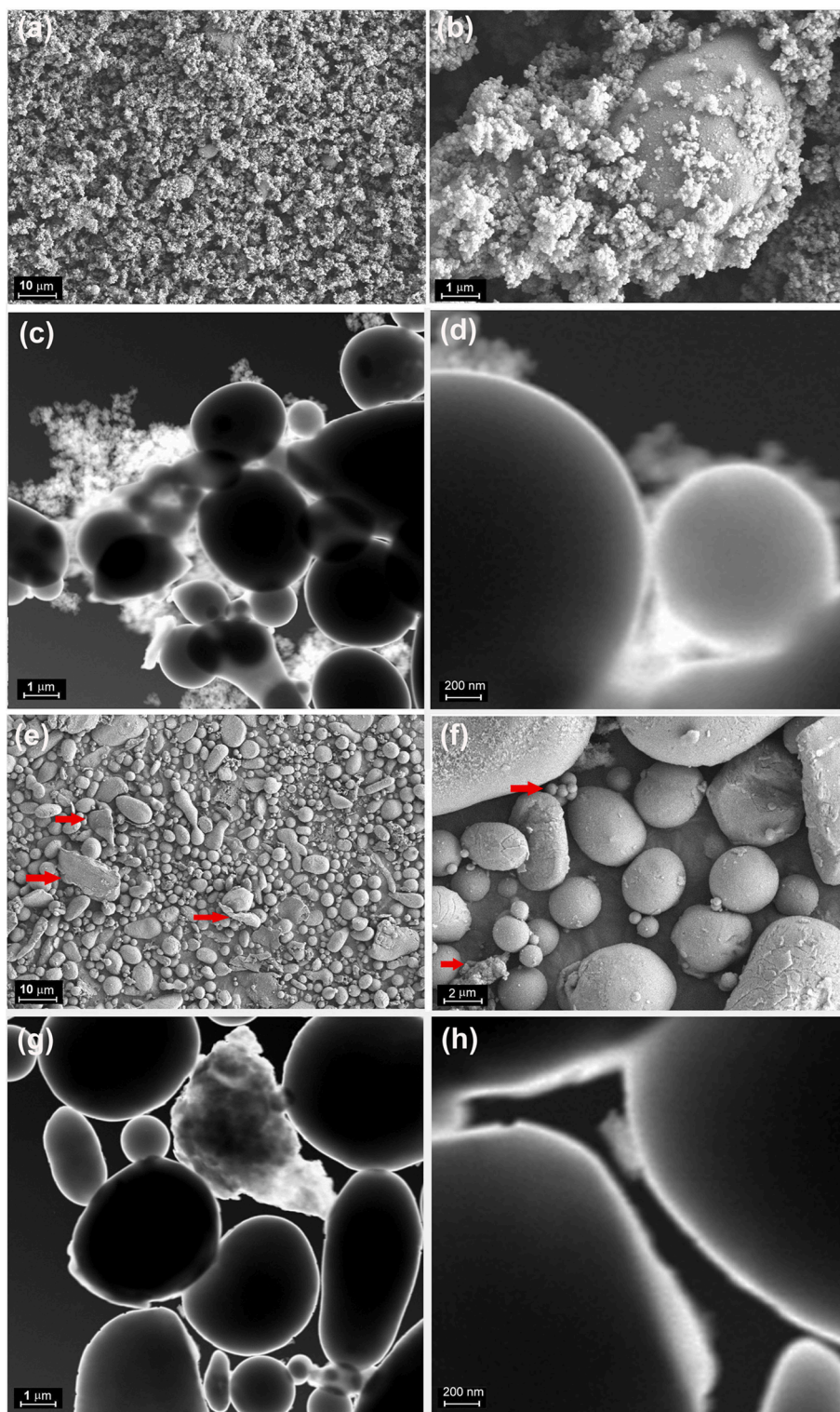
Fig. 11. SEM and STEM images of the product obtained via PVP-assisted approach and reverse microemulsion method: (a-d) reverse microemulsion method and (e-f) PVP-assisted approach. Sn type is Sn-I.

3.2.4. A comparison with the traditional Stöber process-based methods

For the sake of comparison, the PVP-assisted approach proposed by Graf et al. [18] and the reverse microemulsion method proposed by Han et al. [19] were also employed to encapsulate Sn microparticles (Sn-I) in SiO$_2$ (Note: the microemulsion cannot forms in our experiment because the metal particles are micro-sized). To grow a sufficiently thick layer of SiO$_2$ on the nanoparticle surface, a significantly longer reaction time is required in these methods compared to the ultrasound-assisted,

interface-confined sol–gel method. For example, at least 12 h is needed in the PVP-assisted approach (note that this method needs another 24 h for adsorption of PVP on the nanoparticle surface) [18] and over 24 h is required in the reverse microemulsion method [19]. As shown in Fig. 11a-d, there are large amount of free SiO$_2$ nanoparticles in the product prepared by the same procedure as the reverse microemulsion method and many Sn microparticles are partially coated with SiO$_2$. In the product obtained by PVP-assisted method, some sheet-like materials

(indicated by arrows in Fig. 11e) and SiO_2 aggregates (indicated by arrows in Fig. 11f) can be observed, and the STEM images also show that the SiO_2 layer on the particle surfaces is thin and not continuous (Fig. 11g-11 h). These observations suggest that although these time-consuming methods are extremely effective for coating metal nanoparticles with SiO_2 of desired thickness, they are not useful for coating metal microparticles with a uniform SiO_2 layer of desired thickness.

4. Conclusions

In summary, an ultrasound-assisted, interface-confined sol–gel method has been presented for fast encapsulation of metal microparticles in SiO_2. The results have revealed that the assistance of probe sonication and the addition of surfactant are crucial to achieve a dispersion of metal microparticles in cyclohexane that is necessary for efficiently encapsulating microparticles in SiO_2 via interface-confined sol–gel method, and the formation of free SiO_2 can be prevented by using glycerol as the hydrolysis inhibitor, controlling the amount of water and the volume ratio of water to alcohol, and choosing a suitable ultrasonic power. Our results have also shown that the thickness of the SiO_2 layer can be adjusted by changing the reaction time or the total amount of water, especially by simply repeating the encapsulation procedure. In comparison with the traditional Stöber process-based methods, the proposed method is time-saving and extremely effective for encapsulating microparticles of different shapes with a continuous, uniform SiO_2 layer of desired thickness.

CRediT authorship contribution statement

Youwen Tian: Investigation, Methodology, Writing - original draft. **Wei Luo:** Investigation. **Yedan Wang:** Investigation. **Yun Yu:** Investigation. **Wanzhen Huang:** Resources. **Haodong Tang:** Project administration. **Yifan Zheng:** Formal analysis. **Zongjian Liu:** Conceptualization, Funding acquisition, Writing - review & editing.

Declaration of Competing Interest

The authors declare that they have no known competing financial interests or personal relationships that could have appeared to influence the work reported in this paper.

Acknowledgments

References

[1] S.H. Liu, M.Y. Han, Silica-coated metal nanoparticles, Chem. Asian J. 5 (2010) 36–45.
[2] C.Z. Liu, Z.H. Rao, J.T. Zhao, Y.T. Huo, Y.M. Li, Review on nanoencapsulated phase change materials: preparation, characterization and heat transfer enhancement, Nano Energy 13 (2015) 814–826.
[3] I. Pastoriza-Santos, J. Pérez-Juste, L.M. Liz-Marzán, Silica-coating and hydrophobation of CTAB-stabilized gold nanorods, Chem. Mater. 18 (10) (2006) 2465–2467.
[4] Y. Kobayashi, J. Imai, D. Nagao, M. Takeda, N. Ohuchi, A. Kasuya, M. Konno, Preparation of multilayered silica–Gd–silica core-shell particles and their magnetic resonance images, Colloids Surf. A 308 (1-3) (2007) 14–19.
[5] K. Chatterjee, S. Sarkar, K. Jagajjanani Rao, S. Paria, Core/shell nanoparticles in biomedical applications, Adv. Colloid Interface Sci. 209 (2014) 8–39.
[6] T. Zhang, H. Zhao, S. He, K. Liu, H. Liu, Y. Yin, C. Gao, Unconventional route to encapsulated ultrasmall gold nanoparticles for high-temperature catalysis, ACS Nano 8 (7) (2014) 7297–7304.
[7] N. Zanganeh, V.K. Guda, H. Toghiani, J.M. Keith, Sinter-resistant and highly active sub-5 nm bimetallic Au−Cu nanoparticle catalysts encapsulated in SiO_2 for high-temperature carbon monoxide oxidation, ACS Appl. Mater. Interfaces 10 (2018) 4776–4785.
[8] L. Yue, J.M. Li, C. Chen, X.L. Fu, Y. Gong, X.L. Xia, J.W. Hou, C.J. Xiao, X.J. Chen, L.J. Zhao, G.M. Ran, H.Y. Wang, Thermal-stable Pd@mesoporous SiO_2 core-shell nanocatalysts for dry reforming of methane with good coke-resistant performance, Fuel 218 (2018) 335–341.
[9] J. Giro-Paloma, Mònica Martínez, L.F. Cabeza, A.Inés. Fernández, Types, methods, techniques, and applications for microencapsulated phase change materials (MPCM): A review, Renew. Sust. Energ. Rev. 53 (2016) 1059–1075.
[10] T.-H. Hsu, C.-H. Chung, F.-J. Chung, C.-C. Chang, M.-C. Lu, Y.-L. Chueh, Thermal hysteresis in phase-change materials: encapsulated metal alloy core-shell microparticles, Nano Energy 51 (2018) 563–570.
[11] C.-C. Lai, S.-M. Lin, Y.-D. Chu, C.-C. Chang, Y.-L. Chueh, M.-C. Lu, Tunable endothermic plateau for enhancing thermal energy storage obtained using binary metal alloy particles, Nano Energy 25 (2016) 218–224.
[12] K. Kashiyama, T. Kawaguchi, K. Dong, H. Sakai, N. Sheng, A. Kurniawan, T. Nomura, Ga-based microencapsulated phase change material for low-temperature thermal management applications, Energy Storage 2 (5) (2020), https://doi.org/10.1002/est2.v2.510.1002/est2.177.
[13] T. Nomura, C.Y. Zhu, N. Sheng, G. Saito, T. Akiyama, Microencapsulation of metal-based phase change material for high-temperature thermal energy storage, Sci. Rep. 5 (2015) 9117.
[14] J.F. Zhang, C.L. Zhao, J. Tong, R. Tu, Silica-coated micro- and nano-materials: synthesis and applications, J. Chin. Ceram. Soc. 45 (2017) 1410–1420.
[15] G.M. Andrés, P.-J. Jorge, L.M. Luis, Recent progress on SiO_2 coating of nanoparticles and related nanomaterials, Adv. Mater. 22 (2010) 1182–1195.
[16] P. Mulvaney, L.M. Liz-Marzán, M. Giersig, T. Ung, Silica encapsulation of quantum dots and metal clusters, J. Mater. Chem. 10 (6) (2000) 1259–1270.
[17] S. Werner, F. Arthur, Controlled growth of monodisperse SiO_2 spheres in the micron size range, J. Colloid Interface Sci. 26 (1968) 62–69.
[18] C. Graf, D.L.J. Vossen, A. Imhof, A. van Blaaderen, A general method to coat colloidal particles with silica, Langmuir 19 (17) (2003) 6693–6700.
[19] Y. Han, J. Jiang, S.S. Lee, J.Y. Ying, Reverse microemulsion-mediated synthesis of silica-coated gold and silver nanoparticles, Langmuir 24 (11) (2008) 5842–5848.
[20] G.H. Wang, A. Harrison, Preparation of iron particles cofated with SiO_2, J. Colloid Interface Sci. 217 (1999) 203–207.